Biology Direct

RESEARCH Open Access

# Robust SH2 binding affinity indicates minimal SH3-to-SH2 communication in Grb2

Eduarda Santos Ventura[1,2†], Mariana Di Felice[1,2†], Julian Toso[1,2], Valeria Pennacchietti[1,2], Angelo Toto[1,2] and Stefano Gianni[1,2*]

**Abstract**
Growth factor receptor–bound protein 2 (Grb2) is a modular adaptor that links activated receptor tyrosine kinases to downstream signaling pathways through its SH3–SH2–SH3 architecture. Previous studies showed that perturbations in the SH2 domain can influence ligand binding at the C-terminal SH3 domain, suggesting directional allosteric communication within the protein. Here, we tested whether the flanking SH3 domains, in turn, modulate SH2-mediated ligand recognition. Using a parallel mutational scan of the isolated SH2 domain and full-length Grb2, combined with stopped-flow kinetics and double-mutant-cycle analysis, we found that SH2 binding energetics remain essentially unchanged in the presence of the SH3 domains. Only three of twenty-one variants displayed measurable coupling, and none exceeded the threshold typically associated with significant allosteric effects. Pre-binding of the C-SH3 domain to a Gab2-derived peptide likewise produced no detectable influence on SH2–ligand binding. These results reveal a marked asymmetry in interdomain communication in Grb2 and show that the SH2 domain functions as a robust, largely autonomous module within the full-length protein.

**Keywords** Adaptor proteins, Kinetics, Allostery, Site-directed mutagenesis

## Introduction

Growth factor receptor–bound protein 2 (Grb2) is a central adaptor protein that orchestrates the formation of signaling complexes downstream of activated receptors. Although it does not possess any catalytic activity, its ability to assemble protein networks with high precision allows the efficient transmission of extracellular signals to intracellular pathways [1, 2].

Grb2 participates in multiple signaling cascades initiated by receptor tyrosine kinases (RTKs), most notably the Ras–MAPK pathway, which regulates cell growth, differentiation, and survival [3, 4]. Altered expression or malfunction of Grb2 has been associated with oncogenic processes, underscoring the importance of understanding the molecular principles that govern its function [5–8].

Grb2 adopts a conserved tri-domain structure composed of a central Src homology 2 (SH2) domain flanked by N- and C-terminal Src homology 3 (SH3) domains. Through this modular architecture, the SH2 domain recognizes phosphorylated tyrosine motifs (typically pY–X–N), while the SH3 domains bind proline-rich sequences such as those present in Son of Sevenless (SOS) [9–11]. Although these domains can act independently, growing evidence indicates that modular signaling proteins

†Eduarda Santos Ventura and Mariana Di Felice contributed equally to this work.

*Correspondence:
Stefano Gianni
stefano.gianni@uniroma1.it
[1]Dipartimento di Scienze Biochimiche "A. Rossi Fanelli", Sapienza Università di Roma, Rome 00185, Italy
[2]Fondazione Cenci Bolognetti, Laboratory affiliated to Istituto Pasteur Italia, Rome, Italy

frequently rely on subtle energetic communication between domains to coordinate their activities [12, 13].

Understanding whether such communication exists requires a careful and systematic evaluation of all possible pathways through which conformational or energetic signals might propagate [14]. Allosteric analysis therefore demands not only examining direct structural contacts but also quantifying how perturbations in one domain influence the binding properties of another [15–18]. In Grb2, previous work has revealed that mutations in the SH2 domain can modulate binding at the C-SH3 domain, demonstrating that interdomain signaling can occur in the SH2 to SH3 direction [19, 20].

Whether the reverse communication pathway exists, however, remains unresolved. If the SH3 domains influence SH2-mediated ligand recognition, such coupling could reflect a bidirectional allosteric network coordinating the assembly of signaling complexes. Alternatively, the SH2 domain may maintain greater energetic robustness in this direction, acting as a relatively insulated module even within the full-length protein.

In this study, we investigate this question by probing how the flanking SH3 domains affect SH2 binding to its physiological partner. Using kinetic binding measurements combined with double mutant cycle analysis, we compare isolated SH2 variants with the corresponding mutations introduced into full-length Grb2. This approach enables a quantitative assessment of interdomain energetic coupling and allows us to determine whether the SH2 domain behaves as a largely autonomous module or participates in a bidirectional allosteric network within Grb2 [21–23].

Our findings reveal that, unlike the previously observed SH2 to SH3 communication, the reverse SH3 to SH2 direction exhibits only minimal allosteric influence. The SH2 domain therefore displays a notable degree of energetic robustness within the full-length protein, maintaining largely autonomous binding behavior despite the presence or engagement of the flanking SH3 domains.

## Materials and methods

### Protein expression and purification

The Grb2 full-length and SH2 isolated domain constructs and all the site-directed variants with N-terminal His tag were inserted into pET28b + plasmid vectors and expressed in *Escherichia coli* BL21 (DE3) cells. Following an overnight culture, 10 mL of BL21 cells were used to inoculate 1 L of LB media conditioned with 30 µg/mL Kanamycin. Bacterial cultures were subsequently incubated at 37 °C with constant agitation (180 rpm); when an absorbance of 0.7 to 0.8 at 600 nm was reached, 1 mM IPTG was added. The cultures were cooled to 25 °C for 24 h to induce protein expression, and cells were then collected by centrifugation. Bacterial pellets were resuspended in 50 mM Tris-HCl buffer, 0.3 M NaCl, pH 7.5, and 10 mM imidazole with the addition of antiprotease tablets (Complete EDTA-free, Roche) and lysed by sonication. Cellular debris were removed by centrifugation at 11 000 rpm for 45 min at 4 °C, and the soluble fractions were loaded onto a nickel-charged HisTrap Chelating HP (GE Healthcare) column equilibrated with 50 mM Tris-HCl, 0.3 M NaCl, pH 7.5, and 10 mM imidazole. The proteins were eluted with a gradient from 10 mM to 1 M imidazole by using an AKTA-prime system and, after collection, the buffer was exchanged to 50 mM Tris-HCl, 0.3 M NaCl, pH 7.5, by using a HiTrap Desalting column (GE Healthcare). Protein concentrations were estimated by measuring the absorbance of tryptophan residue at 280 nm and calculated through the Beer-Lambert equation.

The peptide mimicking the region of SHP2 530 to 551 (EEEQKSKRKGHE**pY**TNIKYSLAD) and the peptide mimicking the region of Gab2 503 to 524 (YSRGSEIQPPPVNRNLKPDRKAK) were purchased from Genscript Biotech Corp (purity > 90%).

### Stopped-flow binding experiments

Kinetic binding experiments were conducted using a single-mixing SX-18 stopped-flow instrument from Applied Photophysics. Changes in fluorescence emission were monitored during the experiments, which were conducted at 10 °C in pseudo-first order condition, by rapidly mixing a constant concentration of protein (WT and variants, 1 µM) versus increasing concentrations of peptide ($SHP2_{530-551}$ and $Gab2_{503-524}$, ranging from 2 to 12 µM). The SH2 domain contains in fact two tryptophan residues at positions 60 and 121. The displacement method was used to obtain the dissociation rate constant of the system under study. In this method, a solution of a preformed complex of protein and peptide was rapidly mixed with an excess competitor ligand. The buffer used in all experiments was 50 mM Hepes, 0.5 M NaCl at pH 7.0. The final concentration for Grb2 Full-length, SH2 isolated construct and all variants was typically 1 µM.

The samples were excited at 280 nm, and the fluorescence emission light was recorded with a 320 nm cutoff glass filter. Typically for all binding and displacement reactions, five individual traces were averaged and then fitted to a single exponential equation to calculate the observable rate constant. Dependences of $k_{obs}$ as a function of the concentration of peptide were fitted with the following linear equation:

$$k_{obs} = k_{on}\,[\text{Peptide}] + k_{off} \tag{1}$$

Fluorescence signals were detected using a photomultiplier tube, and the absolute voltage values of the traces depend on the instrumental gain settings rather than

representing absolute fluorescence intensities. For this reason, kinetic analyses were based exclusively on relative fluorescence changes. Inspection of the kinetic traces indicates that the fluorescence variation associated with binding and unbinding corresponds to more than 10% of the intrinsic protein fluorescence. Importantly, all measurements displayed an excellent signal-to-noise ratio, allowing reliable single-exponential fitting of the kinetic traces. Differences in absolute fluorescence amplitude between the isolated SH2 domain and full-length Grb2 therefore do not affect the determination of kon, koff, or their associated standard deviations.

## Results

To investigate whether the flanking SH3 domains modulate the ligand-binding properties of the central SH2 domain, we designed a comparative mutational scanning strategy. Our approach relied on generating a parallel set of site-directed variants in two structural contexts: the isolated SH2 domain and full-length Grb2. By examining how identical mutations influence binding in each construct, we aimed to quantitatively assess the contribution of SH3-to-SH2 energetic communication. Accordingly, we expressed and purified wild-type Grb2 full-length, the isolated SH2 domain, and a comprehensive panel of single-site variants in both constructs. Each protein was characterized using stopped-flow fluorescence kinetics to determine the association and dissociation rate constants for binding to a peptide derived from SHP2 (residues 530–551). Association rate constants ($k_{on}$) were assessed by rapidly mixing a fixed concentration of protein (1μM) with increasing concentrations (ranging from 2 to 12 μM) of a peptide mimicking SHP2 from residues 530 to 551 ($SHP2_{530-551}$) and dissociation rate constants ($k_{off}$) were obtained using a displacement method, as described in the experimental section.

All kinetic traces were fitted to an exponential equation to retrieve the observable rate constant of each binding reaction ($k_{obs}$) as shown in Fig. 1. In all cases, a single exponential decay could satisfactorily fit the data. Calculated rate constant were plotted as a function of the different concentrations of $SHP2_{530-551}$ and data was analyzed using a linear equation (Eq. 1 in the experimental section). The slope and y-axis intercept correspond, respectively, to the microscopic association ($k_{on}$) and dissociation ($k_{off}$) rate constants and the affinity of the interaction was calculated as $K_D=k_{off}/k_{on}$.

### Binding properties of SH2 domain in isolation with $SHP2_{530-551}$

23 site-directed variants of SH2 domain in isolation were expressed and purified as described in the experimental section; and subjected to binding experiments described above. As classically adopted in allosteric and energetic-coupling studies, our mutational strategy relied on introducing minimal, conservative substitutions designed to probe local contributions without substantially perturbing the global fold. Accordingly, we selected side-chain variations such as Ile→Val, Thr→Ser, Phe→Ala, Tyr→Ala, Leu→Ala and Ala→Gly. These mutations reduce or subtly alter local packing while preserving the overall structural integrity of the SH2 domain. Applying this same set of perturbations to both the isolated SH2 construct and the full-length Grb2 protein enabled a direct comparison of energetic effects in the two contexts, thereby allowing us to identify residues whose contributions are sensitive to the presence of the flanking SH3 domains. Figure 2 shows the dependences of the binding interaction of SH2 domain variants in the context of the isolated domain in comparison with the wild-type construct. Table 1 synthesizes the binding kinetic data retrieved from the mentioned experiments.

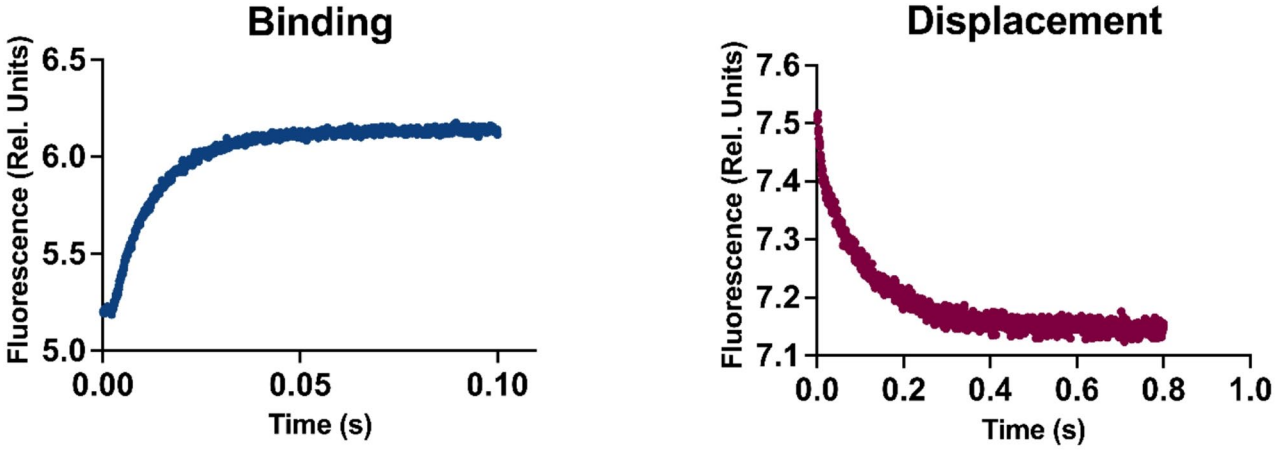


**Fig. 1** Kinetic binding experiments of the SH2 Domain in isolation. Left panel – Binding trace of SH2 (1 μM) with SHP2 (12μM). Right panel – Displacement trace of the preformed complex SH2-SHP2 against a competitor peptide SHP2-Dansyl

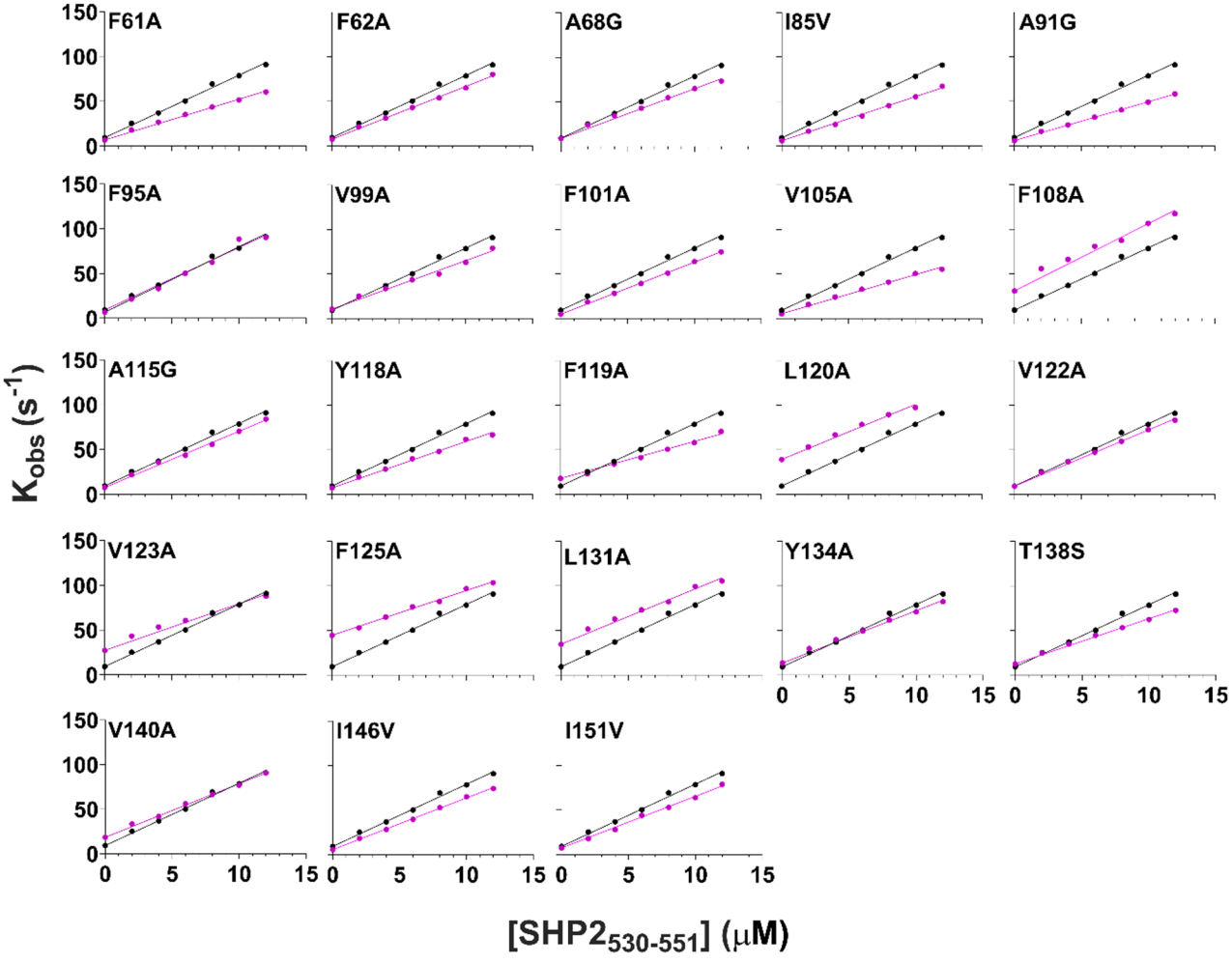


**Fig. 2** Kinetic parameters of the binding reaction of SH2 domain in isolation and its site-directed mutants with $SHP2_{530-551}$. Dependences of $k_{obs}$ values of the binding interaction between the SH2 domain in isolation, both WT (black) and 23 site-directed variants (fuchsia) with different concentrations of $SHP2_{530-551}$. Lines represent the best fit to Eq. 1

### Binding properties of Grb2 Full-length with $SHP2_{530-551}$

To understand the impact of the flanking SH3 domains on the binding interaction of SH2 with $SHP2_{530-551}$, we expressed and purified the same site-directed variants of SH2 domain, this time in the full-length construct of Grb2. The mutants were expressed and purified as described in the experimental section and subjected to binding experiments described above. Figure 3 shows the dependences of the binding interaction of the SH2 domain and variants, in the context of the full-length protein. Table 2 synthesizes the binding kinetic data retrieved from the mentioned experiments.

### Double mutant cycle analysis

With the purpose of quantitatively characterize the energetic coupling between the residues of Grb2 that interfere with the binding of SH2 domain to the SHP2-like peptide, we resorted to conduct a double mutant cycle analysis (DMC). The double-mutant cycle approach is a powerful method for quantifying the strength of molecular interactions between side chains. This technique relies on the combination of site-directed mutagenesis and quantitative analysis of the biophysical properties of a protein system. In DMC analysis two residues are mutated separately and in combination; and the effects of the mutations on the free energy of some processes (e.g. folding, binding or catalysis) are measured. The difference between the effect of the double mutation, and the sum of effects of the two single mutations provides a measure of the energetic coupling (ΔΔΔG) between the two residues [24–26].

The ΔΔΔG is calculated following the equation:

$$\Delta\Delta\Delta G = \Delta\Delta G^{double\ mutation} - \Delta\Delta G^{single\ mutation} - \Delta\Delta G^{single\ mutation}$$

**Table 1** Kinetic parameters of the binding reaction of SH2 domain in isolation with $SHP2_{530-551}$

| SH2 Isolated Domain | | | | |
|---|---|---|---|---|
| | $k_{on\ (}\mu M^{-1}s^{-1})$ | $k_{off}$ ($s^{-1}$) | $K_D$ (μM) | ΔΔG (kcal $mol^{-1}$) |
| WT | 7 ± 0.1 | 9.3 ± 0.1 | 1.33 ± 0.02 | - |
| F61A | 4.55 ± 0.07 | 6.74 ± 0.04 | 1.48 ± 0.02 | 0.06 ± 0.01 |
| F62A | 5.93 ± 0.07 | 7.48 ± 0.03 | 1.26 ± 0.02 | -0.03 ± 0.01 |
| I65V* | - | - | - | - |
| A68G | 5.60 ± 0.13 | 8.89 ± 0.06 | 1.59 ± 0.04 | 0.10 ± 0.02 |
| A70G* | - | - | - | - |
| L84A* | - | - | - | - |
| I85V | 4.95 ± 0.07 | 6.03 ± 0.05 | 1.22 ± 0.02 | -0.05 ± 0.01 |
| A91G | 4.35 ± 0.04 | 5.95 ± 0.03 | 1.37 ± 0.01 | 0.02 ± 0.01 |
| F95A | 7.3 ± 0.2 | 6.8 ± 0.8 | 0.9 ± 0.1 | -0.20 ± 0.07 |
| L97A* | - | - | - | - |
| V99A | 5.44 ± 0.15 | 10.6 ± 0.4 | 1.95 ± 0.09 | 0.21 ± 0.03 |
| F101A | 5.84 ± 0.05 | 4.89 ± 0.03 | 0.84 ± 0.01 | -0.26 ± 0.01 |
| V105A | 4.39 ± 0.08 | 5.39 ± 0.03 | 1.23 ± 0.02 | -0.04 ± 0.01 |
| F108A | 7.5 ± 0.3 | 30.8 ± 0.3 | 4.1 ± 0.2 | 0.63 ± 0.02 |
| L111A* | - | - | - | - |
| A115G | 6.3 ± 0.1 | 7.50 ± 0.08 | 1.20 ± 0.02 | -0.06 ± 0.02 |
| Y118A | 5.2 ± 0.1 | 7.2 ± 0.1 | 1.38 ± 0.04 | 0.02 ± 0.02 |
| F119A | 4.1 ± 0.1 | 18.0 ± 0.2 | 4.3 ± 0.1 | 0.66 ± 0.02 |
| L120A | 6.2 ± 0.2 | 39.1 ± 0.6 | 6.3 ± 0.2 | 0.87 ± 0.02 |
| V122A | 6.30 ± 0.08 | 9.12 ± 0.05 | 1.45 ± 0.02 | 0.05 ± 0.01 |
| V123A | 5.2 ± 0.2 | 27.3 ± 0.3 | 5.2 ± 0.2 | 0.77 ± 0.02 |
| F125A | 5.0 ± 0.1 | 44.6 ± 0.5 | 8.9 ± 0.2 | 1.07 ± 0.02 |
| L131A | 6.2 ± 0.2 | 34.6 ± 0.4 | 5.6 ± 0.2 | 0.80 ± 0.02 |
| Y134A | 5.9 ± 0.1 | 13.5 ± 0.1 | 2.30 ± 0.05 | 0.31 ± 0.02 |
| T138S | 5.08 ± 0.07 | 12.60 ± 0.08 | 2.48 ± 0.04 | 0.35 ± 0.01 |
| V140A | 6.01 ± 0.08 | 18.5 ± 0.4 | 3.08 ± 0.08 | 0.47 ± 0.02 |
| I146V | 5.80 ± 0.05 | 5.72 ± 0.06 | 0.99 ± 0.01 | -0.17 ± 0.01 |
| I151V | 5.8 ± 0.1 | 7.58 ± 0.05 | 1.31 ± 0.02 | -0.01 ± 0.01 |

* These mutants were poorly expressed and could not be characterized

Hence, we quantified coupling free energies (ΔΔΔG) obtained from binding experiments involving the variants of Grb2 full-length. Specifically, the double mutant comprises both a protein truncation and a site-specific mutation, whereas the single mutants correspond either to the truncation alone or to a site-directed mutation introduced in the Grb2 wild-type. Figure 4 provides a simplified sketch to understand the mutations in the double mutant cycle. All variants were analyzed in complex with the $SHP2_{530-551}$ peptide.

The calculated ΔΔΔG values obtained from the binding interaction of SH2 domain variants and $SHP2_{530\text{-}551}$ peptide are reported in Table 3. A value of ΔΔΔG = 0 represents that the mutated residues in the SH2 domain are not influenced by the flanking C-SH3 and N-SH3 domains during binding to the $SHP2_{530\text{-}551}$ peptide, whereas a value of ΔΔΔG ≠ 0 indicates that the mutated residues in the SH2 domain are affected by the adjacent domains. Figure 5 (A) compares the ΔΔG measured upon mutation of the isolated SH2 domain versus the full-length protein construct. It is evident that the data set is consistent with a linear behavior and most of the mutants are consistent with a line starting at the origin and displaying a slope of 1. The only mutants that deviate from this line are F62A, which is located at the interface between SH2 and C-SH3; and F108, F119, V123, and F125, which are located very close to the binding site, as shown in Fig. 5 (B).

We observed small perturbations in most residues, and only 3 of 21 residues (F62, F119, and F125) presented a significant value of ΔΔΔG upon mutation (in the case of binding experiments performed by stopped-flow analysis, it was shown previously that a reliable value of ΔΔΔG should exceed the quantity of ≥0.4 kcal $mol^{-1}$, which represents a conservative threshold well above the experimental uncertainty in stopped-flow–based double mutant cycle analyses.) [27, 28].

In the present dataset, the standard deviations associated with ΔΔΔG values are typically in the range of ±0.02–0.06 kcal $mol^{-1}$ (Table 3). Accordingly, the ±0.4 kcal $mol^{-1}$ threshold corresponds to a signal that is at least 6–15 times larger than the experimental uncertainty. Even if a more permissive criterion based on 2 SD (≈0.1–0.15 kcal $mol^{-1}$) were adopted, the overall conclusions would remain unchanged, as the vast majority of residues would still display minimal coupling and no extended allosteric network would emerge.

### Probing the effect of C-SH3 ligands on the contiguous SH2 domain

In our previous work, we demonstrated that the C-SH3 domain of Grb2 is capable of sensing the binding state of the adjacent SH2 domain, revealing a clear allosteric communication pathway in the **SH2 → C-SH3** direction(20). This raised the question of whether this communication is bidirectional or instead asymmetric—i.e., whether the central SH2 domain is similarly influenced by the binding state of its flanking SH3 domains.

To address this, we set out to test the opposite direction of communication, examining whether occupancy of the C-SH3 domain affects the ligand-binding properties of the SH2 domain. To do so, we compared previously acquired kinetic data for full-length Grb2 binding to the $SHP2_{530–551}$ peptide with new experiments in which the C-SH3 domain was placed in a bound state using a peptide mimicking its physiological ligand $Gab2_{503–524}$. A schematic representation of this experimental design is shown in Fig. 6 (A).

We considered the variants that present a different behavior when comparing the isolated domain construct versus the full-length Grb2, namely: F62A, F108A, F119A, V123A, and F125A (Fig. 6 (B)). The pseudo-first order binding plots of these mutants in the presence and in absence of a saturating concentration of $Gab2_{503\text{-}524}$ are

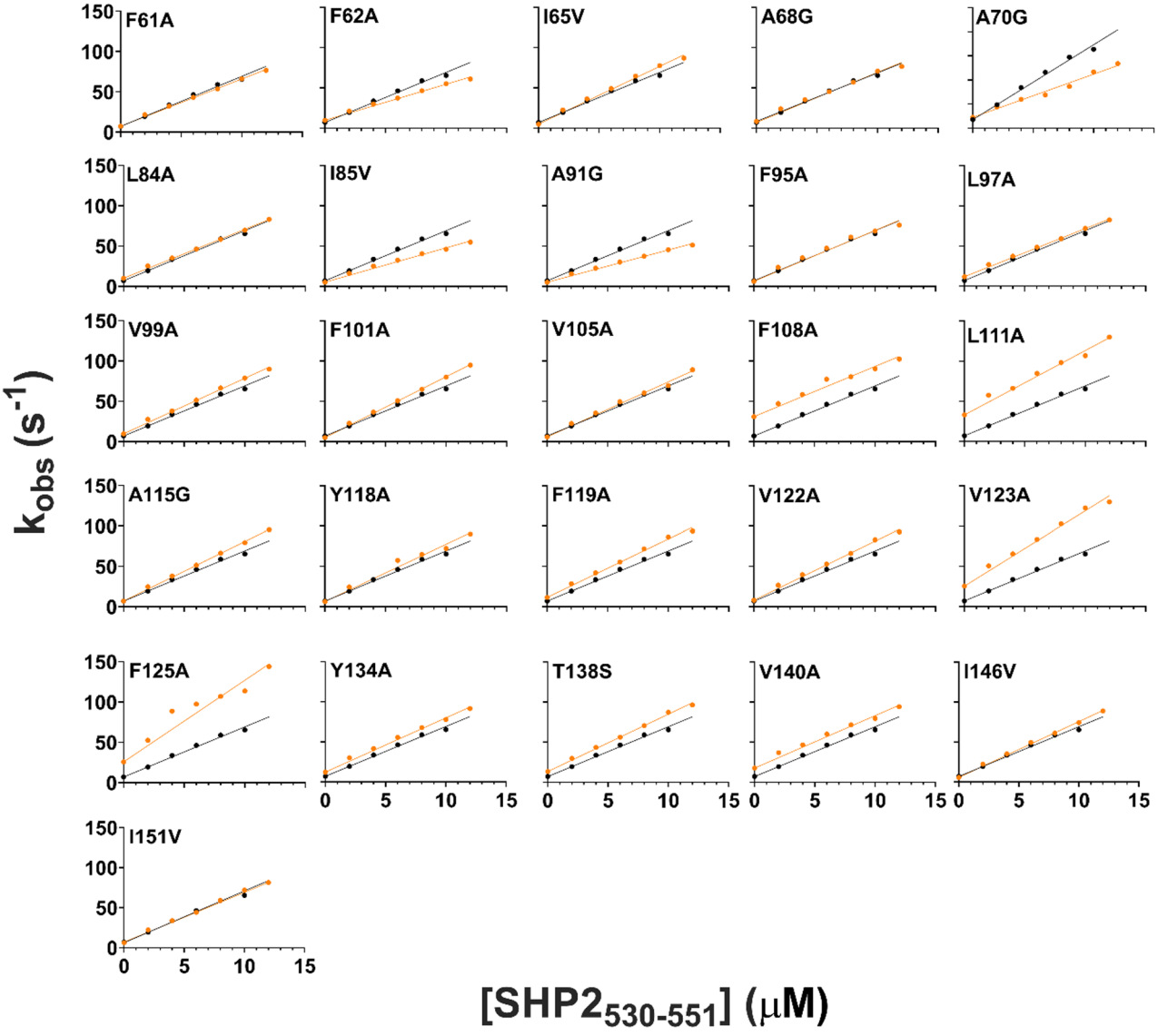


**Fig. 3** Kinetic parameters of the binding reaction of SH2 of Grb2 full length and its site-directed mutants with SHP2$_{530-551}$. Dependences of $k_{obs}$ values of the binding interaction between Grb2 WT (black) and 26 site-directed variants of the SH2 domain (orange) in the context of the full-length protein, with different concentrations of SHP2$_{530-551}$. Lines represent the best fit to Eq. 1

reported in Fig. 6 (B) and the calculated parameters are reported in Table 4.

In contrast with our earlier finding, the present dataset shows no comparable influence of the SH3 domains on SH2-mediated binding. Every single-site mutation probed in the full-length construct produced kinetic and thermodynamic parameters that closely matched those obtained for the isolated SH2 domain. Importantly, in the presence of Gab2$_{503-524}$, none of the ΔΔG values approached or exceeded the established threshold of 0.4 kcal mol$^{-1}$, the conventional criterion for meaningful allosteric coupling in stopped-flow double-mutant cycles. The near-identity of $k_{on}$, $k_{off}$, and $K_D$ values across all variants further supports the absence of any measurable energetic communication transmitted from the SH3 domains to the SH2 binding interface. Taken together, these results indicate that, at variance with the previously observed communication from SH2 to C-SH3, the reverse SH3 → SH2 direction is essentially silent, highlighting a clear asymmetry and a remarkable degree of energetic robustness of the SH2 domain in its native tripartite context.

## Discussion

Scaffolding and adaptor proteins are central organizers of intracellular communication, ensuring that signaling reactions occur with spatial and temporal precision. Their modular architecture—typically composed of

**Table 2** Kinetic parameters of the binding reaction of Grb2 Full-length WT and variants with $SHP2_{530-551}$

| Grb2 Full Length | | | | |
|---|---|---|---|---|
| | $k_{on}$ ($\mu M^{-1}s^{-1}$) | $k_{off}$ ($s^{-1}$) | $K_D$ ($\mu M$) | $\Delta\Delta G$ (kcal $mol^{-1}$) |
| WT | 6.2 ± 0.1 | 7.00 ± 0.06 | 1.13 ± 0.03 | - |
| F61A | 5.86 ± 0.07 | 7.30 ± 0.03 | 1.24 ± 0.02 | 0.06 ± 0.02 |
| F62A | 4.5 ± 0.1 | 9.72 ± 0.04 | 2.17 ± 0.04 | 0.37 ± 0.02 |
| I65V | 7.2 ± 0.1 | 4.90 ± 0.07 | 0.68 ± 0.02 | -0.28 ± 0.02 |
| A68G | 6.0 ± 0.1 | 8.30 ± 0.05 | 1.38 ± 0.03 | 0.11 ± 0.02 |
| A70G | 3.6 ± 0.1 | 8.98 ± 0.05 | 2.51 ± 0.08 | 0.45 ± 0.02 |
| L84A | 6.07 ± 0.07 | 10.10 ± 0.05 | 1.67 ± 0.02 | 0.22 ± 0.02 |
| I85V | 4.3 ± 0.1 | 5.23 ± 0.02 | 1.23 ± 0.03 | 0.05 ± 0.02 |
| A91G | 4.00 ± 0.08 | 5.17 ± 0.02 | 1.29 ± 0.03 | 0.08 ± 0.02 |
| F95A | 6.3 ± 0.2 | 6.35 ± 0.03 | 1.01 ± 0.03 | -0.06 ± 0.02 |
| L97A | 6.00 ± 0.08 | 11.80 ± 0.08 | 1.97 ± 0.03 | 0.31 ± 0.02 |
| V99A | 6.9 ± 0.1 | 9.74 ± 0.08 | 1.42 ± 0.03 | 0.13 ± 0.02 |
| F101A | 7.55 ± 0.07 | 5.00 ± 0.03 | 0.66 ± 0.01 | -0.30 ± 0.02 |
| V105A | 6.8 ± 0.1 | 5.80 ± 0.04 | 0.85 ± 0.02 | -0.16 ± 0.02 |
| F108A | 6.2 ± 0.2 | 31.1 ± 0.7 | 5.0 ± 0.2 | 0.83 ± 0.03 |
| L111A | 8.02 ± 0.20 | 33.0 ± 0.5 | 4.1 ± 0.1 | 0.73 ± 0.02 |
| A115G | 7.40 ± 0.08 | 7.06 ± 0.03 | 0.96 ± 0.01 | -0.09 ± 0.02 |
| Y118A | 7.1 ± 0.3 | 6.4 ± 0.1 | 0.90 ± 0.04 | -0.13 ± 0.03 |
| F119A | 7.2 ± 0.1 | 11.6 ± 0.1 | 1.60 ± 0.03 | 0.20 ± 0.02 |
| L120A* | - | - | - | - |
| V122A | 7.3 ± 0.1 | 8.06 ± 0.05 | 1.10 ± 0.02 | -0.01 ± 0.02 |
| V123A | 9.4 ± 0.2 | 25.4 ± 0.2 | 2.71 ± 0.07 | 0.49 ± 0.02 |
| F125A | 10.1 ± 0.6 | 25.7 ± 2.2 | 2.5 ± 0.3 | 0.46 ± 0.06 |
| L131A* | - | - | - | - |
| Y134A | 6.8 ± 0.1 | 12.2 ± 0.1 | 1.80 ± 0.04 | 0.26 ± 0.02 |
| T138S | 7.2 ± 0.1 | 13.2 ± 0.1 | 1.84 ± 0.03 | 0.28 ± 0.02 |
| V140A | 6.5 ± 0.2 | 17.5 ± 0.3 | 2.7 ± 0.1 | 0.48 ± 0.02 |
| I146V | 7.0 ± 0.1 | 5.68 ± 0.02 | 0.81 ± 0.01 | -0.18 ± 0.02 |
| I151V | 6.5 ± 0.1 | 6.30 ± 0.07 | 0.98 ± 0.02 | -0.08 ± 0.02 |

* These mutants were poorly expressed and could not be characterized

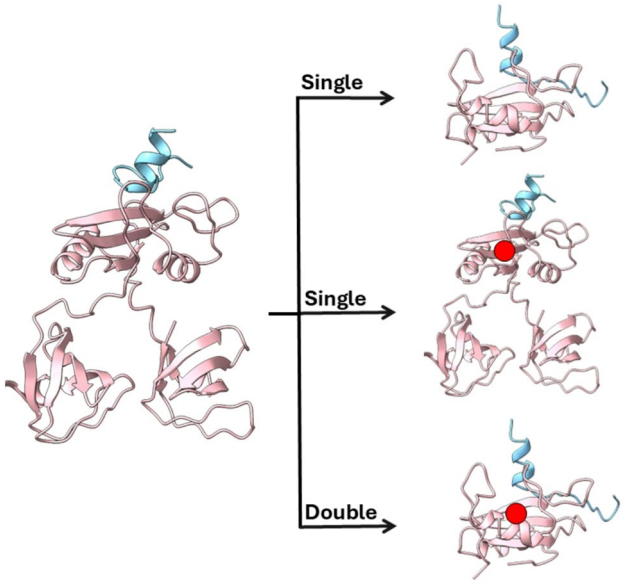


**Fig. 4** Double mutant cycle for the SH2 domain of Grb2–peptide interaction. As described in the text, starting from full-length Grb2: one single mutation is the protein truncation (SH2 domain in isolation), the other single mutation is the site-specific mutation in full-length Grb2 (red dot), and the double mutation is both the protein truncation and the site-specific mutation. The binding site of SH2 domain with SHP2 was simulated with AlphaFold, and the image was created with UCSF Chimera

**Table 3** Coupling free energies ($\Delta\Delta\Delta G$) of SH2 domain variants

| Mutants | $\Delta\Delta\Delta G$ (kcal $mol^{-1}$) |
|---|---|
| F61A | 0.00 ± 0.02 |
| F62A | 0.40 ± 0.02 |
| A68G | 0.01 ± 0.03 |
| I85V | 0.10 ± 0.02 |
| A91G | 0.06 ± 0.02 |
| F95A | 0.14 ± 0.08 |
| V99A | -0.09 ± 0.03 |
| F101A | -0.04 ± 0.02 |
| V105A | -0.11 ± 0.02 |
| F108A | 0.20 ± 0.04 |
| A115G | -0.03 ± 0.02 |
| Y118A | -0.15 ± 0.03 |
| F119A | -0.46 ± 0.03 |
| V122A | -0.06 ± 0.02 |
| V123A | -0.27 ± 0.03 |
| F125A | -0.61 ± 0.06 |
| Y134A | -0.04 ± 0.02 |
| T138S | -0.07 ± 0.02 |
| V140A | 0.01 ± 0.03 |
| I146V | -0.02 ± 0.02 |
| I151V | -0.07 ± 0.02 |

independently folded domains linked by flexible or semi-rigid connectors—allows them to integrate multiple inputs while distributing outputs to diverse downstream pathways [29–31].

Grb2 exemplifies this design principle: through its SH2 and dual SH3 domains, it nucleates the assembly of receptor-proximal signaling complexes and couples phosphorylated receptors to Ras activation. Understanding whether these domains operate independently or communicate energetically is therefore fundamental not only for elucidating the biophysics of Grb2 itself but also for understanding how signaling networks leverage modularity to achieve specificity and robustness [19, 20, 32].

In this context, our study examined how the flanking SH3 domains influence the binding interaction mediated by the central SH2 domain. Although allosteric interactions have been described within multi-domain signaling proteins, the extent of interdomain communication can vary dramatically, ranging from strongly cooperative to functionally insulated [33–39]. Prior work on Grb2 demonstrated that the SH2 domain can modulate binding of the C-SH3 domain, suggesting that the protein may possess inherent allosteric circuitry [19, 20]. Here, by interrogating the reverse direction of information flow, we sought to determine whether the SH3 domains

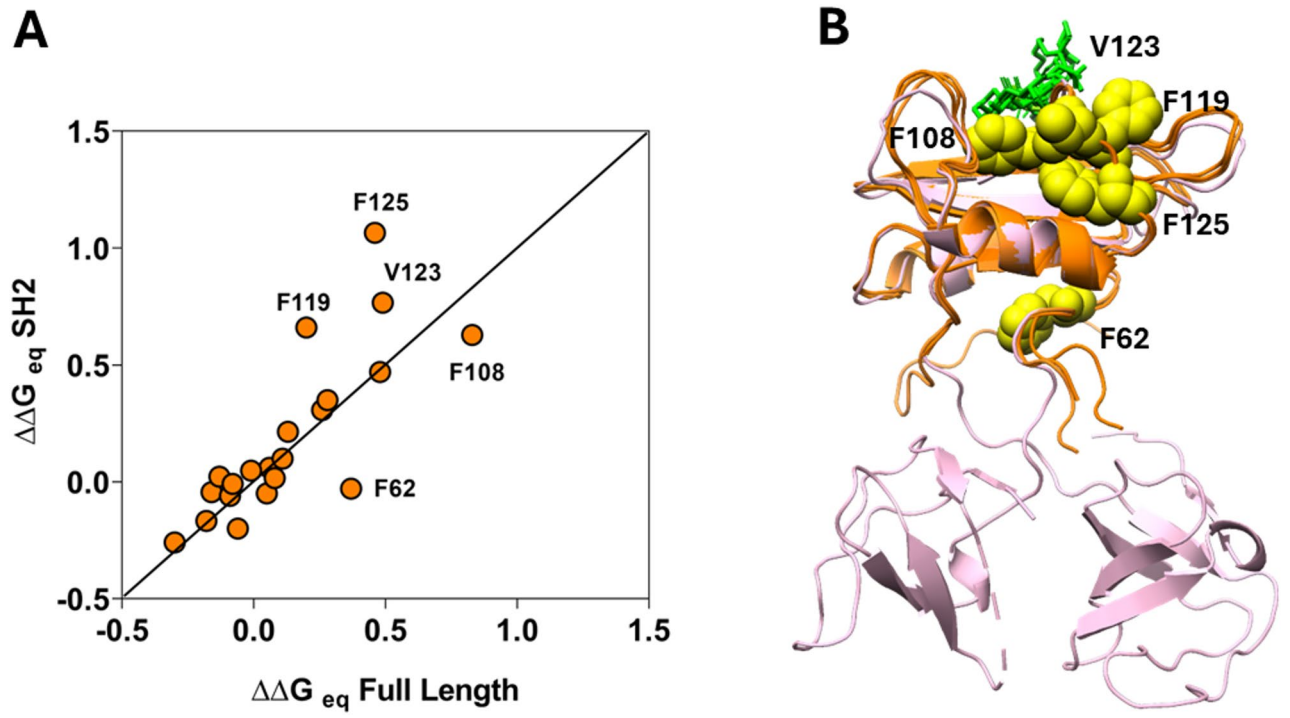


**Fig. 5** Comparison between the variants of the isolated SH2 domain and the full-length Grb2. **(A)** Comparison of the $\Delta\Delta G_{eq}$ values upon mutation for the isolated SH2 domain versus the full-length protein. **(B)** On the right, the cartoon representation, created with USCF Chimera, of sequence alignment of the full-length Grb2 protein (PDB: 1GRI) and the SH2 domain bound to pY-X-N containing sequences (where X denotes any amino acid, and N denotes asparagine) (PDB: 3N7Y, 1CJ1, 3N84). Structural distribution of the residues (highlighted in yellow on the SH2 domain structure) that have a different behavior upon mutation on the isolated domain compared to the full-length protein

reciprocally tune SH2-mediated ligand recognition. Our kinetic data indicate that, for the majority of SH2 residues examined, binding to the SHP2-derived peptide is minimally affected by the presence of the adjacent SH3 domains. This observation situates Grb2 within a class of adaptor proteins whose domains retain substantial energetic autonomy, despite being arranged in close proximity [19, 20]. Such autonomy may be advantageous in signaling contexts where domains must bind partners independently or in a sequential manner without imposing unnecessary energetic constraints on one another [40].

Nevertheless, our results also reveal discrete points of communication. Double mutant cycle analysis identified three residues—F62, F119, and F125—that exhibit significant coupling free energies when comparing the isolated SH2 domain to the full-length protein. These positions cluster at the SH2/C-SH3 interface or near the ligand-binding pocket, regions structurally poised to mediate interdomain interactions. Their sensitivity suggests that interdomain communication in Grb2 is not globally distributed but transmitted through specific residues that act as conduits of energetic coupling. This pattern reflects an emerging principle in modular proteins: allosteric effects often propagate through sparse, evolutionarily conserved networks rather than through wholesale rearrangements of the domain [32, 41, 42]. The comparison between ΔΔG values in the isolated versus full-length constructs further underscores this idea. The strongly linear relationship across most variants indicates that the SH2 domain largely behaves as an independent folding and binding module. Deviations from this linearity highlight the residues where domain–domain interactions exert measurable influence, aligning with the coupling energies observed in the double mutant cycles [26].

We also explored whether occupation of the C-SH3 domain by its physiological partner Gab2 enhances or reshapes this communication. In some signaling proteins, ligand binding at one domain induces conformational changes or shifts in domain orientation that influence the activity of adjacent modules. Under our experimental conditions, however, engagement of the C-SH3 domain produced only subtle effects on SH2 binding energetics. No variant exhibited a ΔΔG exceeding the threshold typically associated with meaningful allosteric modulation in stopped-flow experiments. These modest changes suggest either that SH3 engagement does not substantially perturb SH2 function or that a more complex multivalent or membrane-associated environment—one that more closely mimics the cellular context—may be required to reveal stronger coupling. We note that a higher fraction

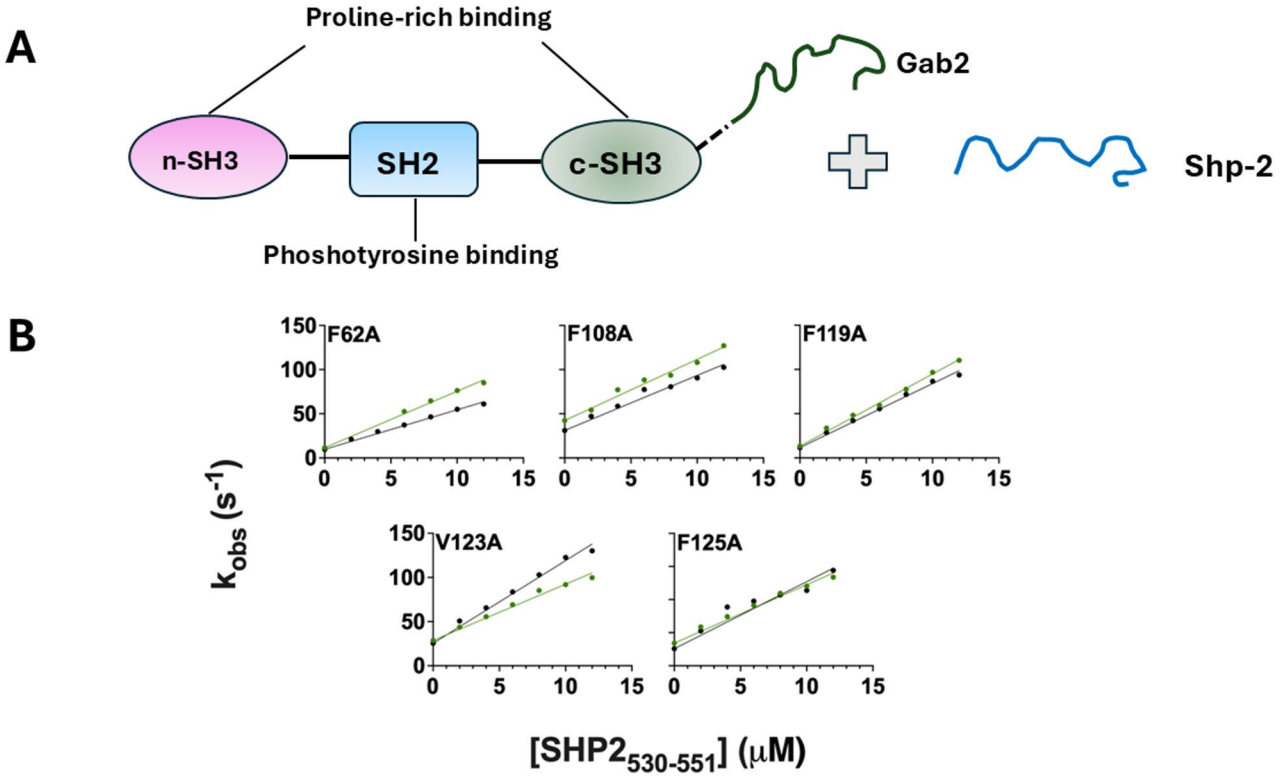


**Fig. 6** Kinetic binding experiments between Grb2 and a peptide mimicking SHP2 in absence or in presence of Gab2$_{503-524}$. **(A)** A schematic representation of the stopped-flow experiments performed in this study: full-length Grb2 protein with its physiological SH2 domain ligand, SHP2$_{530-551}$. The C-SH3 domain was pre-bound to Gab2$_{503-524}$, a peptide mimicking its physiological partner. (**B**) Kinetic experiments were performed on mutants that show different behavior between the isolated SH2 domain and the full-length protein, in the absence (black) and presence (dark green) of Gab2$_{503-524}$

**Table 4** Kinetic parameters of the binding reaction of Grb2 FL variants with SHP2$_{530-551}$ in the presence of Gab2$_{503-524}$

| **Grb2 Full Length variants in presence of Gab2$_{503-524}$** | | | | |
|---|---|---|---|---|
| | $k_{on}$ (μM$^{-1}$s$^{-1}$) | $k_{off}$ (s$^{-1}$) | $K_D$ (μM) | ΔΔG (kcal mol$^{-1}$) |
| F62A | 6.4 ± 0.1 | 11.50 ± 0.08 | 1.80 ± 0.04 | 0.11 ± 0.02 |
| F108A | 6.9 ± 0.2 | 42.3 ± 2.0 | 6.1 ± 0.3 | -0.11 ± 0.04 |
| F119A | 8.2 ± 0.1 | 13.2 ± 0.1 | 1.62 ± 0.03 | -0.01 ± 0.02 |
| V123A | 6.4 ± 0.2 | 28.6 ± 0.4 | 4.5 ± 0.1 | -0.28 ± 0.02 |
| F125A | 8.8 ± 0.3 | 34.1 ± 0.3 | 3.9 ± 0.1 | -0.24 ± 0.06 |

of poorly expressed or unstable mutants was observed in regions of the SH2 domain enriched in α-helical structure compared to β-sheet regions. This behavior likely reflects stricter structural constraints in the helical segments, which play a key role in maintaining the overall fold and stability of the SH2 domain and are therefore less tolerant to even conservative substitutions. Importantly, this reduced mutational tolerance should not be directly interpreted as evidence of reduced allosteric potential, but rather as a consequence of local stability requirements. Accordingly, the limited allosteric coupling observed in SH2 is more appropriately attributed to energetic robustness than to structural rigidity.

Taken together, our findings position Grb2 as a predominantly modular adaptor in which the SH2 domain maintains robust autonomy but retains specific points of interdomain sensitivity. This hybrid architecture—mostly independent but selectively interconnected—may reflect the competing demands of signaling fidelity and regulatory flexibility [9, 43]. Autonomous domains allow Grb2 to interact with distinct partners simultaneously, while limited communication could enable context-dependent fine-tuning of affinity, especially in crowded cellular environments or upon formation of higher-order signaling assemblies.

Overall, this work contributes a quantitative description of how energetic communication is distributed within Grb2 and underscores the importance of considering both domain independence and selective crosstalk when interpreting the behavior of multi-domain signaling proteins. Future studies incorporating additional ligands, multivalent complexes, or structural dynamics approaches may further illuminate how these subtle energetic couplings contribute to the broader logic of signal transduction.

#### Author contributions

E.S.V., M.D.F. and S.G. designed research. E.S.V., M.D.F., J.T., V.P. and A.T. performed research. All authors analyzed data. E.S.V., M.D.F. and S.G. wrote the first version of the manuscript. All authors read and accepted the manuscript.

**Funding**
This work was partly supported by grants from European Union's MSCA Doctoral Networks under the Grant Agreement IDPro No 101119633 (to S.G.), by grants from Sapienza University of Rome (RG12017297FA7223, RG1231888A88129D to S.G., RG124190E53A81B8, RM12218148DA1933 to A.T.), the Associazione Italiana per la Ricerca sul Cancro (Individual Grant—IG 24551 to S.G.), the Istituto Pasteur Italia ("Research Program 2022 to 2023 Under 45 Call 2020" to A.T.), the Italian MUR-PRIN 2022 grant N. 2022JY3PMB to A.T. We acknowledge co-funding from Next Generation EU, in the context of the National Recovery and Resilience Plan, and the Investment PE8—Project Age-It: "Ageing Well in an Ageing Society". The views and opinions expressed are only those of the authors and do not necessarily reflect those of the European Union or the European Commission. Neither the European Union nor the European Commission can be held responsible for them.

**Data availability**
No datasets were generated or analysed during the current study.

## Declarations

**Ethical approval**
Not applicable.

**Competing interests**
The authors declare no competing interests.

Received: 16 December 2025 / Accepted: 14 January 2026
Published online: 23 January 2026

**References**

1. Malagrinò F, Puglisi E, Pagano L, Travaglini-Allocatelli C, Toto A. GRB2: A dynamic adaptor protein orchestrating cellular signaling in health and disease. Biochem Biophys Rep. 2024;39:101803.
2. Chardin P, Cussac D, Maignan S, Ducruix A. The Grb2 adaptor. FEBS Lett. 1995;369(1):47–51.
3. Lowenstein EJ, Daly RJ, Batzer AG, Li W, Margolis B, Lammers R, et al. The SH2 and SH3 domain-containing protein GRB2 links receptor tyrosine kinases to Ras signaling. Cell. 1992;70(3):431–42.
4. Egan SE, Giddings BW, Brooks MW, Buday L, Sizeland AM, Weinberg RA. Association of Sos Ras exchange protein with Grb2 is implicated in tyrosine kinase signal transduction and transformation. Nature. 1993;363(6424):45–51.
5. Daly RJ, Binder MD, Sutherland RL. Overexpression of the Grb2 gene in human breast cancer cell lines. Oncogene. 1994;9(9):2723–7.
6. Li H, Zhang Y, Han X, Li B, Liu D, Sun G. GRB2 promotes brain metastasis in HER2-positive breast cancer by regulating the Ras/MAPK pathway. Sci Rep. 2025;15(1):14736.
7. Wang D, Liu G, Meng Y, Chen H, Ye Z, Jing J. The configuration of GRB2 in protein interaction and signal transduction. Biomolecules. 2024;14(3):259.
8. Li Z, Zhao PL, Gao X, Li X, Meng YQ, Li ZQ, et al. DUS4L suppresses invasion and metastasis in LUAD via modulation of PI3K/AKT and ERK/MAPK signaling through GRB2. Int Immunopharmacol. 2024;142:113043.
9. Tateno K, Ando T, Tabata M, Sugasawa H, Hayashi T, Yu S, et al. Different molecular recognition by three domains of the full-length GRB2 to SOS1 proline-rich motifs and EGFR phosphorylated sites. Chem Sci. 2024;15(38):15858–72.
10. Waksman G, Kominos D, Robertson SC, Pant N, Baltimore D, Birge RB, et al. Crystal structure of the phosphotyrosine recognition domain SH2 of v-src complexed with tyrosine-phosphorylated peptides. Nature. 1992;358(6388):646–53.
11. Lim WA, Richards FM, Fox RO. Structural determinants of peptide-binding orientation and of sequence specificity in SH3 domains. Nature. 1994;372(6504):375–9.
12. Chartier CA, Woods VA, Xu Y, van Vlimmeren AE, Johns AC, Jovanovic M, et al. Allosteric regulation of the tyrosine phosphatase PTP1B by a protein–protein interaction. Protein Sci. 2025;34(1).
13. Jasemi NSK, Ahmadian MR. Allosteric regulation of GRB2 modulates RAS activation. Small GTPases. 2022;13(1):282–6.
14. Montserrat-Canals M, Cordara G, Krengel U, Allostery. Q Rev Biophys. 2025;58:e5.
15. Guo J, Zhou HX. Protein allostery and conformational dynamics. Chem Rev. 2016;116(11):6503–15.
16. Cooper A, Dryden DTF. Allostery without conformational change. Eur Biophys J. 1984;11(2):103–9.
17. Nussinov R, Wolynes PG. A second molecular biology revolution? The energy landscapes of biomolecular function. Phys Chem Chem Phys. 2014;16(14):6321.
18. Gunasekaran K, Ma B, Nussinov R. Is allostery an intrinsic property of all dynamic proteins? Proteins Struct Funct Bioinform. 2004;57(3):433–43.
19. Di Felice M, Pagano L, Pennacchietti V, Diop A, Pietrangeli P, Marcocci L, et al. The binding selectivity of the C-terminal SH3 domain of Grb2, but not its folding pathway, is dictated by its contiguous SH2 domain. J Biol Chem. 2024;300(4):107129.
20. Di Felice M, Rolfi LR, Toso J, Pennacchietti V, Ventura ES, Toto A, et al. Allosteric modulation of Grb2 drives ligand-dependent signal responses. Biol Direct. 2025;20(1):63.
21. Laursen L, Kliche J, Gianni S, Jemth P. Supertertiary protein structure affects an allosteric network. Proc Natl Acad Sci. 2020;117(39):24294–304.
22. Nardella C, Pagano L, Pennacchietti V, Di Felice M, Di Matteo S, Diop A, et al. An intramolecular energetic network regulates ligand recognition in a SH2 domain. Protein Sci. 2023;32(8).
23. Gianni S, Haq SR, Montemiglio LC, Jürgens MC, Engström Å, Chi CN, et al. Sequence-specific long range networks in PSD-95/Discs Large/ZO-1 (PDZ) domains tune their binding selectivity. J Biol Chem. 2011;286(31):27167–75.
24. Horovitz A, Fleisher RC, Mondal T. Double-mutant cycles: new directions and applications. Curr Opin Struct Biol. 2019;58:10–7.
25. Carter PJ, Winter G, Wilkinson AJ, Fersht AR. The use of double mutants to detect structural changes in the active site of the tyrosyl-tRNA synthetase (Bacillus stearothermophilus). Cell. 1984;38(3):835–40.
26. Pagano L, Toto A, Malagrinò F, Visconti L, Jemth P, Gianni S. Double mutant cycles as a tool to address Folding, Binding, and allostery. Int J Mol Sci. 2021;22(2):828.
27. Serrano L, Horovitz A, Avron B, Bycroft M, Fersht AR. Estimating the contribution of engineered surface electrostatic interactions to protein stability by using double-mutant cycles. Biochemistry. 1990;29(40):9343–52.
28. Schreiber G, Fersht AR. Energetics of protein-protein interactions: analysis ofthe Barnase-Barstar interface by single mutations and double mutant cycles. J Mol Biol. 1995;248(2):478–86.
29. DiRusso CJ, Dashtiahangar M, Gilmore TD. Scaffold proteins as dynamic integrators of biological processes. J Biol Chem. 2022;298(12):102628.
30. Pawson T. Dynamic control of signaling by modular adaptor proteins. Curr Opin Cell Biol. 2007;19(2):112–6.
31. Huber M, Brummer T. Enzyme is the Name—Adapter is the game. Cells. 2024;13(15):1249.
32. Malagrinò F, Troilo F, Bonetti D, Toto A, Gianni S. Mapping the allosteric network within a SH3 domain. Sci Rep. 2019;9(1):8279.
33. Fedoroff OY, Townson SA, Golovanov AP, Baron M, Avis JM. The structure and dynamics of tandem WW domains in a negative regulator of Notch Signaling, suppressor of Deltex. J Biol Chem. 2004;279(33):34991–5000.
34. Macias MJ, Wiesner S, Sudol M, WW. SH3 domains, two different scaffolds to recognize proline-rich ligands. FEBS Lett. 2002;513(1):30–7.
35. Laursen L, Gianni S, Jemth P. Dissecting Inter-domain cooperativity in the folding of a multi domain protein. J Mol Biol. 2021;433(18):167148.
36. Macauley MS, Errington WJ, Schärpf M, Mackereth CD, Blaszczak AG, Graves BJ, et al. Beads-on-a-string, characterization of ETS-1 sumoylated within its flexible N-terminal sequence. J Biol Chem. 2006;281(7):4164–72.
37. Trujillo U, Vázquez-Rosa E, Oyola-Robles D, Stagg LJ, Vassallo DA, Vega IE, et al. Solution structure of the tandem acyl carrier protein domains from a polyunsaturated fatty acid synthase reveals Beads-on-a-String configuration. PLoS ONE. 2013;8(2):e57859.
38. Sekine S ichi, Ehara H, Kujirai T, Kurumizaka H. Structural perspectives on transcription in chromatin. Trends Cell Biol. 2024;34(3):211–24.
39. Arrías PN, Monzon AM, Clementel D, Mozaffari S, Piovesan D, Kajava AV, et al. The repetitive structure of DNA clamps: an overlooked protein tandem repeat. J Struct Biol. 2023;215(3):108001.
40. Pawson T, Gish GD, Nash P. SH2 domains, interaction modules and cellular wiring. Trends Cell Biol. 2001;11(12):504–11.
41. Soltan Ghoraie L, Burkowski F, Zhu M. Sparse networks of directly coupled, polymorphic, and functional side chains in allosteric proteins. Proteins. 2015;83(3):497–516.
42. Reynolds KA, McLaughlin RN, Ranganathan R. Hot spots for allosteric regulation on protein surfaces. Cell. 2011;147(7):1564–75.

43. Kazemein Jasemi NS, Herrmann C, Magdalena Estirado E, Gremer L, Willbold D, Brunsveld L, et al. The intramolecular allostery of GRB2 governing its interaction with SOS1 is modulated by phosphotyrosine ligands. Biochem J. 2021;478(14):2793–809.

## Publisher's note